Cancer Letters 442 (2019) 213–221

Contents lists available at ScienceDirect

Cancer Letters

journal homepage: www.elsevier.com/locate/canlet

Original Articles

Progression from low- to high-grade in a glioblastoma model reveals the pivotal role of immunoediting

Irene Appolloni[a], Francesco Alessandrini[a], Davide Ceresa[a], Daniela Marubbi[a,b], Eleonora Gambini[a], Daniele Reverberi[b], Fabrizio Loiacono[b], Paolo Malatesta[a,b,*]

[a] Department of Experimental Medicine (DIMES), University of Genoa, Via Leon Battista Alberti 2, 16132, Genoa, Italy
[b] IRCCS Ospedale Policlinico San Martino, Largo Rosanna Benzi 10, 16132, Genoa, Italy

ARTICLE INFO

Keywords:
Glioblastoma
Immunoediting
Retroviral induced glioma model
Tumor progression
PDGF-B

ABSTRACT

The mutual reshape of tumor and immune system cells during tumor progression is a widely accepted notion in different cancers including gliomas. The importance of this phenomenon in shaping glioma progression and the mechanisms governing it, however, are not fully elucidated. Taking advantage of a well-characterized in vivo glioma model we performed an analysis of glioma cells transcriptomes at different stages of progression and unveiled the reorganization of glioma-immune system interactions. Specifically, we show that the inability of low-grade glioma cells to orthotopically graft in syngeneic immunocompetent mice, positively correlates with the abundance of infiltrating lymphocytes in donor tumors and with a highly immunostimulatory transcriptional profile. Notably, during tumor progression glioma cells downregulate these genes and the immune infiltrate shifts towards a pro-tumorigenic phenotype. Challenging low-grade gliomas by grafting into immunodeficient hosts revealed the crucial role of the adaptive immune system in constraining glioma progression. Finally, we observed that although progression still takes place in immunodeficient mice, it is slower, likely due to a milder selection thus reinforcing the view of a pivotal role for the immune system in regulating glioma progression.

1. Introduction

The concept of a dual role for the immune system during cancer progression defined as immunoediting by Dunn and collaborators [1] has been strengthened in the last 15 years thanks to the work of different laboratories. Data from different tumor types in humans and in animal models demonstrated the existence of all the three phases of tumor immunoediting as extensively reviewed [2–5]. Evidences for the first phase (Elimination), in which the immune system actively counteracts tumor growth, derived from the observations that immunodeficient mice as well as immunosuppressed patients have a higher incidence of tumors. Moreover, it has been shown that the presence of tumor-infiltrating lymphocytes (TIL), especially CD8-positive cells, often correlates with a favorable prognosis in different tumor types. The second phase consists of a period of tumor latency, which in humans can last many years, during which a dynamic equilibrium is established between the host immune system and tumor cells. This equilibrium phase was deduced in humans by the existence of occult cancers that become clinically manifest only after transplantation in an immunosuppressed recipient [3,4]. More direct evidence for the role of the adaptive system in controlling cancer growth came from a mouse model of occult sarcomas driven by exposure to low doses of 3-methylcholanthrene [6]. In the final phase, tumor cells increase growth rates following successful escape from immune system surveillance. Immunoediting is thus a central feature of the tumorigenic process and reflects stage-specific interactions between the immune system and tumor cells. This is often characterized by a strong early negative selection and later co-option of tumor-promoting mechanisms [3,4,7,8]. Further evidence for this mechanism comes from the fact that tumors emerging in immunodeficient mice are more immunogenic than those arising in immunocompetent animals [9–11].

In the case of gliomas, the idea of an active role for the immune system during tumorigenesis is relatively recent, due to the long-held view of this organ as an immune-privileged compartment almost isolated from immune cells. It is now clear however, that the brain is immune-competent and permissive to immune cells infiltration and therefore more appropriately defined as immunologically distinct [2,12,13]. In this scenario, the model of tumor immunoediting was proposed also for gliomas and several glioma antigens as well as many mechanisms for immune evasion have been defined both in humans and in animal models [2,8]. All these data reveal the existence of the 3 phases of immunoediting in gliomas and highlight the translational

* Corresponding author. Department of Experimental Medicine (DIMES), University of Genoa, Via Leon Battista Alberti 2, 16132, Genoa, Italy.
E-mail address: paolo.malatesta@unige.it (P. Malatesta).

https://doi.org/10.1016/j.canlet.2018.10.006
Received 28 May 2018; Received in revised form 8 September 2018; Accepted 4 October 2018

importance of a comprehensive understanding of this process. A crucial point is to study how tumor and immune cells change their phenotype during glioma progression but the current animal models based on transplantation of highly immunogenic and in vitro selected glioma cell lines [14] do not allow to elucidate this aspect.

In this work, by exploiting a well-established model of glioma progression driven by the in vivo overexpression of the PDGF-B oncogene [15,16], we obtained for the first time a direct evidence of a progressive change in the behavior of both immune system and glioma cells. This phenomenon recapitulates the immunoediting process, leading a tumor from the elimination to the escape phase. In particular, we showed that during the first steps of tumorigenesis, glioma cells are highly immunogenic. In later stages they downregulate immunostimulatory genes and reshape the phenotype of immune system cells that acquire an anti-inflammatory, pro-tumorigenic M2 phenotype.

Altogether, our data show that the evolution of an immune-escape strategy for glioma cells is crucial for glioma progression.

2. Materials and methods

2.1. Animal procedures

All animal procedures were approved by the internal committee for the protection of animals used for scientific purposes (OPBA) of the Ospedale policlinico San Martino and by the Italian Ministry of Health according to the Italian law D. lgs 26/2014 and the European Directive 2010/63/EU of the European Parliament. In all the experiments were used the C57BL/6J and the NOD.CB17-Prkdc^{scid}/J strains (hereinafter respectively referred as C57BL/6 and NOD/SCID) from Jackson Laboratory.

Intraventricular injections of replication-incompetent retroviral vectors in E14 mouse embryos were performed in deeply anesthetized pregnant females as already described by Terrile and collaborators [17].

Orthotopic transplantations of murine glioma cells in adult mouse brains were performed as described in a previous publication [18]. Depending on the experiments the number of implanted cells ranged from 3×10^3 to 2×10^5.

Tumor masses were visualized by using a Leica fluorescence microscope thanks to the EGFP expression and dissected in HBSS medium (Life Technologies). Tumor cells were dissociated with enzymatic digestion in Trypsin/EDTA and mechanical dissociation with a Pasteur pipette in 10% FBS (Life Technologies). After centrifugation at $500 \times g$ for 5 min, the pellet was suspended in specific media for further processing. For orthotopic transplantation or in vitro culturing tumor cells were suspended in neural stem cell medium: DMEM/F12 and 1X B27 supplement (Life Technologies), 10 ng/ml EGF and 10 ng/ml bFGF (Peprotech). For fluorescent activated cell sorting (FACS) or flow cytometry cells were suspended in PBS supplemented with 1% FBS and 1.5 mM EDTA.

The survival curves were obtained by using the Kaplan-Meier estimator.

2.2. Immunostainings

Mouse brains were fixed overnight in 4% paraformaldehyde in PBS, cryoprotected overnight in 20% sucrose, embedded in Tissue Teck O.C.T. and frozen at −80 °C. Sections were obtained with a Leica CM3050 S cryostat. Sections were permeabilized 30 min with 0.1% Triton X-100 (Bio-Rad) in PBS. Primary antibodies were incubated over-night at 4 °C in PBS with 10% goat serum (Sigma-Aldrich) and 0.1% BSA (Sigma-Aldrich), while secondary antibodies were incubated 1 h at room temperature in PBS and 10% goat serum. For CD206 staining donkey serum instead of goat serum was used. For Arginase I staining, before permeabilization, sections were boiled 3 times in citrate buffer pH 6 for 4 min for antigen retrieval and the subsequent washes were performed using PBS-T solution (0.1% Tween-20 in PBS).

The following primary antibodies were used: chicken polyclonal antisera against GFP (1:500, ab13970 Abcam); rat monoclonal anti-mouse CD8 YTS105.18 clone (1:500, MCA1108GT AbDSerotec); rat monoclonal anti-mouse CD4 RM4-5 clone (1:100, 550280 BD Pharmingen); rabbit polyclonal anti-human MPO (1:300, A0398 Dako); rabbit polyclonal antibodies against Iba1 (1:250, 019–19741 Wako), mouse monoclonal anti-mouse ArginaseI E − 2 clone (1:50, SC-271430 Santa Cruz Biotechnology), goat polyclonal anti-mouse CD206 (1:100, AF2535 R&D System); rabbit polyclonal anti-GranzymeB antibody (1:100, PA1-26616 Thermofisher).

The following secondary antibodies were used: goat anti-chicken Alexa Fluor 488 (1:500, A11039 Molecular Probes), goat anti-rabbit Dylight 549-conjugated AffiniPure (1:500, 111-505-003 Jackson Immunoresearch Laboratories), goat anti-rat Cy3-conjugated AffiniPure (1:500, 112-165-167 Jackson Immunoresearch Laboratories), goat anti-mouse Dylight 549-conjugated AffiniPure (1:500, 115-505-044 Jackson Immunoresearch Laboratories), donkey anti-goat biotin-conjugated (1:50, ab6884 Abcam), streptavidin Alexa Fluor 546-conjugated (1:500, S11225 Molecular Probes). Nuclei were stained with Hoechst 33342 (1 μg/ml, Sigma-Aldrich).

2.3. Image analysis

The analysis of CD4$^-$ CD8-and MPO-positive cells in the brain sections were analyzed by computer-assisted camera-lucida drawings. Briefly, positions on x- and y-axis of immunostained-positive cells and points on the perimeter of brain sections and glioma masses were registered using a Zeiss motorized epifluorescence microscope (Axio Imager.M2) and the AxioVision Rel. 4.8 software (Zeiss, Oberkochen). Data were analyzed with a R script (available on GitHub repository at the website: https://github.com/PaoloMalatesta/LucidaGraph) that automatically draws the images and performes the statistical analyses.

2.4. Flow cytometry

Dissociated cells were suspended in PBS supplemented with 1% FBS and 1.5 mM EDTA, incubated with APC-conjugated monoclonal rat anti-mouse CD45 (1:200, 559864 BD Pharmingen) for 20 min and analyzed with CyAn ADP (Beckman Coulter). For negative control, we used APC-conjugated rat isotype control (1:200, 17432181 eBioscience).

Cell sorting was performed on a FACSAria II (BD Biosciences) with an 85 μm nozzle tip at a default pressure of 45 psi with the highest precision sort mode. Discrimination doublets and checked sorting gate were done with a dot plot where GFP-Area parameter matched with GFP-Width parameter and then monitored in a FSC-A vs SSC-A dot plot.

2.5. Microarray analysis

Dissociated cells from 4 early and 2 late onset tumors were sorted for EGFP with FACSAria II. EGFP-positive cells from 4 independent early onset tumors were pooled in two pools to reach a sufficient amount of cells for further analysis. Cells were harvested in Trizol (Invitrogen) for RNA extraction. Microarray hybridization procedure was performed at the “Consorzio Genopolis” (University of Milano-Bicocca, Dept. of Biotechnology and Bioscience) using the Affymetrix MoGene-1.0-st array (GEO Accession Number GSE108954). RNA extracted from sorted cells from 4 secondary and 3 tertiary tumors obtained by serial transplantation of early onset tumors in NOD/SCID mice were hybridized on Affymetrix GeneChip Mouse Genome 430 2.0 Array (GEO Accession Number GSE108955) by AROS Applied Biotechnology (Aarhus, Denmark). Data were analyzed using the R3.4.0 software and BioConductor version 3.5 [19]. Expression values were extracted from raw data files using the RMA method built in the affy

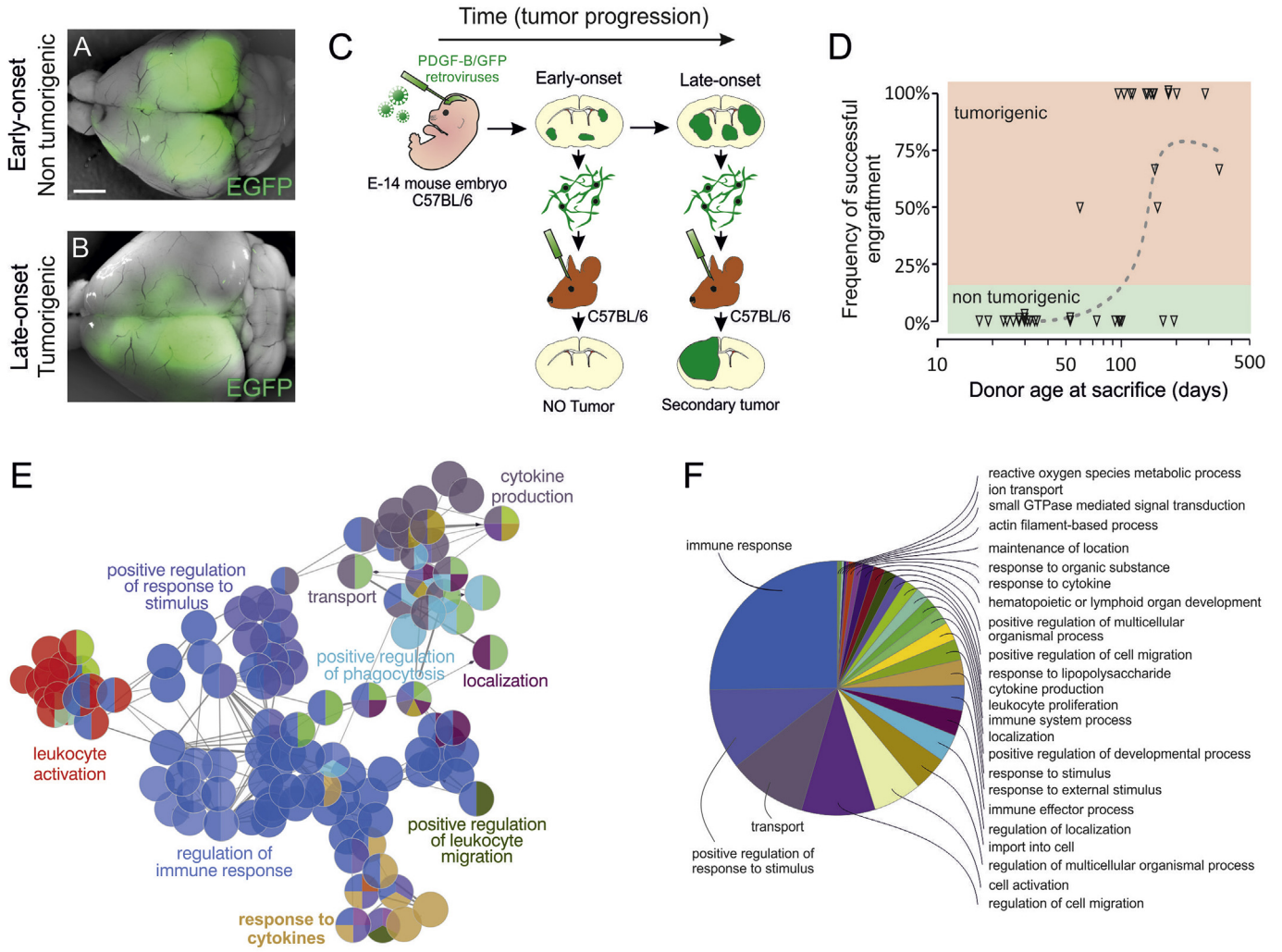

Fig. 1. Functional and molecular characterization of early- and late-onset gliomas. A-B, Merged fluorescence and brightfield images of mouse brains bearing an EGFP-expressing early-onset (A) and a late-onset (B) glioma. Scale bar: 2 mm. C, Experimental scheme for testing the onset of tumorigenic features in glioma cells over time. D, Plot shows the frequency of successful engraftment (i.e. induction of secondary tumors) in syngeneic mice following the transplantation of cells derived from donor showing symptoms at different times (raw data are listed in Supplementary Table 1a). Dashed line represents the trend of the frequency of successful engraftment over the age of donor at sacrifice by showing the smoothed moving average with a frame (period) of 12 consecutive samples. E-F, Annotation enrichment analysis of the set of genes downregulated during progression showing the network of enriched GoTerm (E) and the relative frequency of each GoTerm among all the GoTerms comprising the considered set of genes (F).

1.54.0 library package. Differentially expressed genes were ranked by using RankProd 3.2.0 library. To create the heat map summarizing data derived from different platforms (i.e. MoGene-1.0-st and MouseGenome 430 2.0 arrays) raw data were processed with RMA omitting the normalization step. Probesets referring to the same MGI gene symbol were aggregated for each platform by using geometric means then the dataset were merged basing on gene symbol annotations. The entire dataset was eventually quantile normalized [20] and the heatmap was drawn with R-Core *stats* version 3.5.0. GoTerm enrichment analysis was carried with ClueGO [21] plugin for Cytoscape [22].

3. Results

We generated gliomas by injecting, into the lateral ventricles of E14 embryos, replication-incompetent retroviral vectors expressing the PDGF-B oncogene and the EGFP reporter gene, as previously described [15,16]. Injected animals developed multi-focal gliomas, which induce neurologic symptoms at different time points in their juvenile/adult life (Fig. 1A–B). In accordance with previously published data [16] and as shown in Supplementary Fig. 1 and Supplementary Table 1a, early-onset tumors showed typical histological features of low-grade tumors (diffuse, scarcely cellularized masses), while late-onset tumors displayed typical high-grade glioma features (wide and compact masses with large necrotic areas containing pseudopalisading structures). While the analysis by cell-lineage and proliferation markers such as GFAP, Nestin, PDGFR-alpha, NG2, Olig2, Sox2 and Ki67 failed to show any difference between EGFP-positive cells in early onset- and late-onset tumors, which invariably display an oligodendrocyte progenitor cell-like profile, a striking difference emerges in transplantation assays. EGFP-positive cells dissociated from early-onset gliomas with low-grade phenotype did not generate secondary tumors after orthotopic transplantation in syngeneic mice, while late-onset, high-grade, gliomas are tumorigenic [16].

As demonstrated by systematic orthotropic transplantations in adult syngeneic mice (experimental scheme shown in Fig. 1C), PDGF-B induced gliomas progressively acquired this malignant feature over time. In particular, we found that no secondary glioma is ever generated by the transplantation of up to 30 000 EGFP-positive cells derived from mice showing neurological symptoms before postnatal day 60 (P60; N = 16). The frequency of successful grafting progressively rises with

the age of the donor at the time of death. The cell explanted from the vast majority of the animals showing neurological symptoms after P100 (15 out of 17) generated secondary tumors in at least one recipient (Fig. 1D and Supplementary Table 1a). Successful grafting appeared not to be influenced by the number of transplanted cells in the range from 3000 to 200 000 cells, and a number smaller or equal to 5000 EGFP-positive cells from tumorigenic gliomas were sufficient to generate secondary tumors in 100% of the assays (n = 7). These data, together with previous observations showing that even tumors fated to develop as high-grade are not able to graft if explanted at early stages (< P60) [16], confirm that glioma cells need time to progress toward a full-blown malignant state and that this animal model can be used to study glioma progression in vivo.

In order to dissect the molecular mechanisms underlying glioma progression, we explanted and dissociated both early-onset/low-grade and late-onset/high grade gliomas (hereinafter respectively referred as “low-grade" and “high-grade" gliomas). We purified by FACS the sole glioma cell component thanks to EGFP expression and we performed a microarray analysis to determine their gene expression profile. Cells derived from high-grade tumors were transplanted in syngeneic mice to confirm they comprise a tumorigenic fraction. Differentially expressed genes were identified by RankProduct [23] using as cutoff pfp = 0.05. This analysis resulted in 58 upregulated and 148 downregulated genes during progression. A gene annotation enrichment analysis on GO-TERM was carried on the two sets, using ClueGO [21,22] and DAVID [24,25]. For the set of genes upregulated during progression, the analysis failed to identify strongly enriched functional clusters (Bonferroni corrected P value $< 10^{-4}$; DAVID Enrichment Score over 1.5). Below this threshold, the most significantly enriched groups were related to multicellular organism development and differentiation. On the contrary, the set of genes downregulated during the progression presented a much more coherent picture, with 10 functional clusters well above the 1.5 Enrichment Score threshold. Prominent clusters appeared to be related to immune system response and inflammation, as shown in Fig. 1E–F, suggesting that progression from low-to high-grade gliomas correlates with a downregulation of immunostimulatory genes.

In order to assess potential differences between low- and high-grade gliomas, with respect to their relationship with the immune system, we characterized the infiltrates in section harboring gliomas. The analysis showed a higher infiltration level of CD8 positive lymphocytes in low-grade tumor brains (average density of 26 ± 7 cell/mm^2; n = 13) compared to high-grade tumor or healthy non-transduced brains (one-way ANOVA, p < 0.005). The density of CD8-positive cells in high-grade tumor brains (3.3 ± 1.6 cell/mm^2, n = 8) was not significantly different from healthy non-transduced brains (0.6 ± 0.1 cell/mm ^{2}, n = 8, Fig. 2A–D). On the contrary, the density of CD4-positive lymphocytes does not change during progression (7.2 ± 2.8 cell/mm^2 in the low-grade; 4.9 ± 0.8 cell/mm^2 in the high-grade and 1.1 ± 0.3 cell/mm^2 in healthy brain; not significant, with a power of 0.80 for an effect size ≥1 in a one way anova test; Fig. 2E–H) but their distribution does. While in the low-grade gliomas CD4-positive lymphocytes are evenly distributed between tumor mass and surrounding areas, in high-grade gliomas they are found more frequently inside the tumor mass (p < 0.005; Supplementary Fig. 2B), as often observed in other malignant tumors [26] and in particular in glioblastoma where CD4 TIL are positively correlated with tumor grade [27]. These data show that low-grade, not yet fully progressed gliomas, actively stimulate the specific infiltration of CD8-positive lymphocytes while high-grade gliomas do not. Since it is known that the tumor microenvironment may impair the cytotoxic activity of CD8-positive lymphocytes which then lose granzymeB immunoreactivity [28], we immunostained low-grade tumors with granzymeB and CD8 on adjacent sections. The density of granzymeB-positive cells was compatible with the density of CD8-positive cells suggesting that the majority of CD8 positive lymphocytes retained their cytotoxic activity (Supplementary Fig. 2C and D).

To evaluate whether this difference reflects a different grade in the general inflammation levels, we assessed the percentage of CD45-positive cells by a cytofluorimetric analysis on dissociated tumor masses. The percentage of CD45-positive cells were similar between low- and high-grade tumors (respectively 8.8 ± 0 .1.6% n = 7 and 7.9 ± 0.9% n = 11; Fig. 3A) suggesting that the composition rather than the overall number of immune system cells is different between progressed and unprogressed tumors.

To further characterize the composition of the infiltrates in low- and high-grade gliomas, we looked at innate immune system cells. Immunostainings for Iba1 showed a high presence of microglia-macrophage cells in both low- and high-grade tumors as well as in healthy brains (Fig. 3B–D). These cells displayed an activated microglia amoeboid morphology, regardless of the progression stage in all the analyzed tumors (Fig. 3E and F), in comparison to healthy brains where these cells have a ramified phenotype typical of resting cells (Fig. 3G [29,30]). However, in high-grade gliomas their phenotype appeared associated to alternatively activated M2 immune cells, consistent with an immunomodulatory role. As shown in Fig. 4E–H, high-grade tumors had a high infiltration of immune-modulatory cells expressing CD206 and Arginase-I markers suggesting that progression induced a phenotype switch. Consistent with these observations is also the localization of MPO-positive cells that are significantly enriched in high-grade gliomas in comparison to low-grade (Fig. 4A–D). These cells are found prevalently inside the tumor masses rather than in their periphery, a feature that has been associated with immunomodulatory granulocytes [31]. The overall figure is consistent with the notion that high-grade tumors often recruit M2 macrophages and other immunomodulatory cells in an immune-evasion strategy [7,32].

To test whether there is a difference in the ability to recruit immune system cells, we explanted both low- and high-grade tumors and transplanted them into adult syngeneic mice, evaluating the identity and localization of infiltrated lymphocytes after 2 weeks in brain sections. The time was selected to allow the tissue surrounding the needle tract to recover from the acute nonspecific inflammatory condition induced by the injection itself, although this choice does not allow to take into account earlier events. Both CD8 and CD4 lymphocytes were found at higher density in the brains injected with low-grade gliomas (Fig. 4I–J) where groups of lymphocytes appeared enriched near the tumor injection site.

3.1. Transplantation in immunodeficient mice

We tested whether the inability of low-grade gliomas to give rise to a secondary tumor after orthotopic transplantation depends on their immunostimulatory features. We injected matched aliquots of EGFP-positive cells derived from 5 low-grade gliomas in NOD/SCID immunodeficient mice and, in parallel, in syngeneic C57BL/6 animals (as outlined in Fig. 5A). As expected, no tumor arose in syngeneic mice when the cells were transplanted in 11 C57BL/6 mice and the brains of all these animals appeared completely devoid of EGFP-positive cells. On the contrary, secondary gliomas developed from the cells of 4 out of the 5 independent tumors transplanted in NOD/SCID mice. In total 10 secondary gliomas where obtained from 16 NOD/SCID mice (Fig. 5B, Supplementary Figs. 3–4, Supplementary Table 2). The experiment was further repeated only in NOD/SCID mice with 3 additional independent primary tumors obtaining similar results (2 out of 3 gave rise to secondary gliomas in 3 out of 8 mice; Fig. 5B, Supplementary Figs. 3–4, Supplementary Table 2). These data demonstrated the central role of the adaptive immune system in counteracting tumor grafting and strongly suggested that the growth of low-grade tumors is impaired by the immune system, which therefore may play fundamental roles during the first steps of gliomagenesis.

Interestingly, the analysis of the gene expression profile of cells retrieved from secondary tumors growing in NOD/SCID shows that the set of genes downregulated during progression displays expression

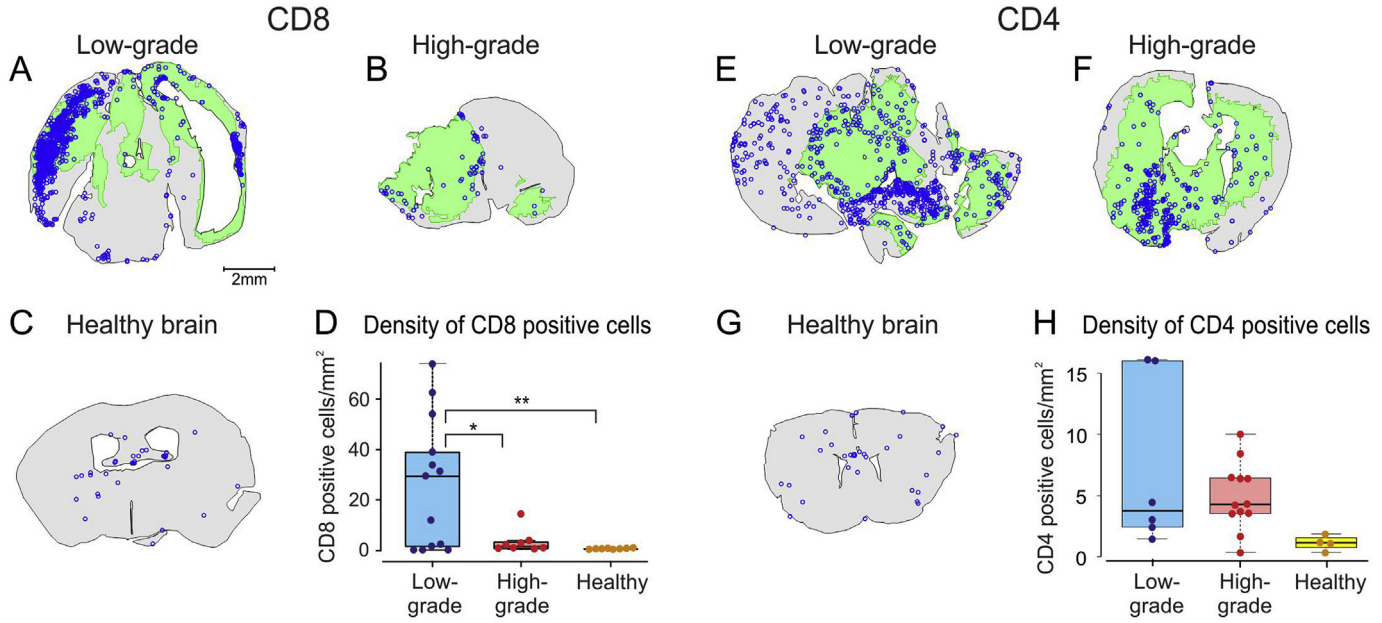

Fig. 2. CD8-and CD4-positve cells infiltration in glioma-bearing brains. A-C, E-G, Computer-assisted camera-lucida drawing of brain sections stained with anti-GFP antibody to label tumor areas (in green) and anti-CD8 (A–C) or anti-CD4 (E–G) antibodies labelling corresponding T-lymphocytes (blue dots). D, H, Histograms show the density of CD8 (D) or CD4 (H) expressing cells in healthy brains or brains bearing low-grade or high-grade gliomas. Statistical analysis was performed by a one-way ANOVA followed by a Tukey HSD post-hoc test (**$p < 0.01$; *$p < 0.05$). Scale bar: 2 mm. (For interpretation of the references to colour in this figure legend, the reader is referred to the Web version of this article.)

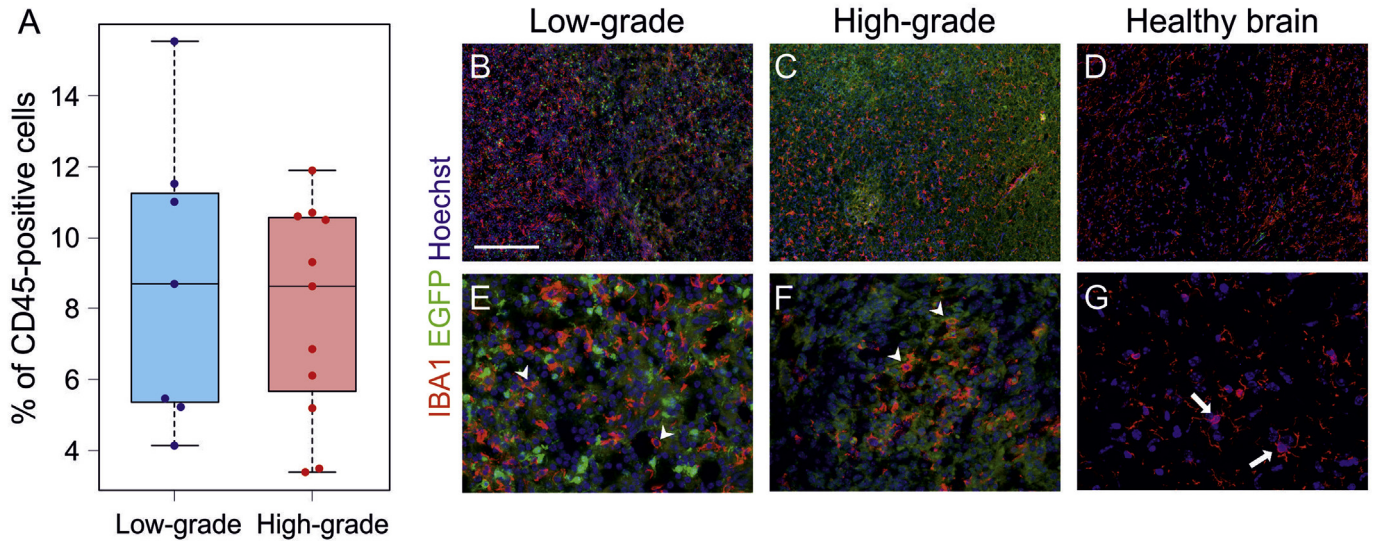

Fig. 3. Analysis of the inflammation level in glioma masses. A, Boxplot showing the percentage of CD45-positive cells infiltrating the tumor mass of low- and high-grade gliomas analyzed by flow cytometry. B-G, show different magnifications of brain sections either harboring low-grade (B,E) or high-grade (C,F) gliomas and normal healthy brain (D,G), immunostained with anti-GFP antibody (in green) labelling tumor cells, anti-Iba1 (in red) labelling microglia and Hoechst 33342 (in blue) labelling nuclei. Arrows show ramified resting cells in the healthy brain (G); arrowheads show activated microglia with short and thick cell processes or amoeboid morphology (E,F) in tumor tissues. Scale bar: 200 μm (B–D), 50 μm (E–G). (For interpretation of the references to colour in this figure legend, the reader is referred to the Web version of this article.)

levels similar to that found in low-grade tumors (Fig. 6A). Secondary gliomas grown in NOD/SCID hosts from low-grade tumors thus appear to retain their original immunostimulatory feature more than high-grade, fully progressed, tumors. This may be due to the much weaker selective pressure imposed by the immunodeficient environment, which may fail to fully reshape the tumor immunophenotype.

However, in some extent, gliomas do eventually progress even in the immunodeficient environment. This is shown by the fact that cells derived from NOD/SCID secondary tumors (4 independent tumors) were able not only to successfully graft in NOD/SCID mice (where all of them gave rise at least to 1 tertiary glioma; in total 8 tertiary gliomas in 11 mice) but, in two cases, also in immunocompetent C57BL/6 mice (generating in total 3 tertiary gliomas in 11 transplanted mice; Fig. 5C, Supplementary Fig. 3, Supplementary Tables 3–4). This observation was unexpected since we anticipated that the immunodeficient environment should not impose a selection based on the glioma cells' immunogenicity, unless for the remnant of immune system present in NOD/SCID.

A hierarchical clustering analysis of the expression profile of the gene set downregulated during progression shows that tertiary gliomas

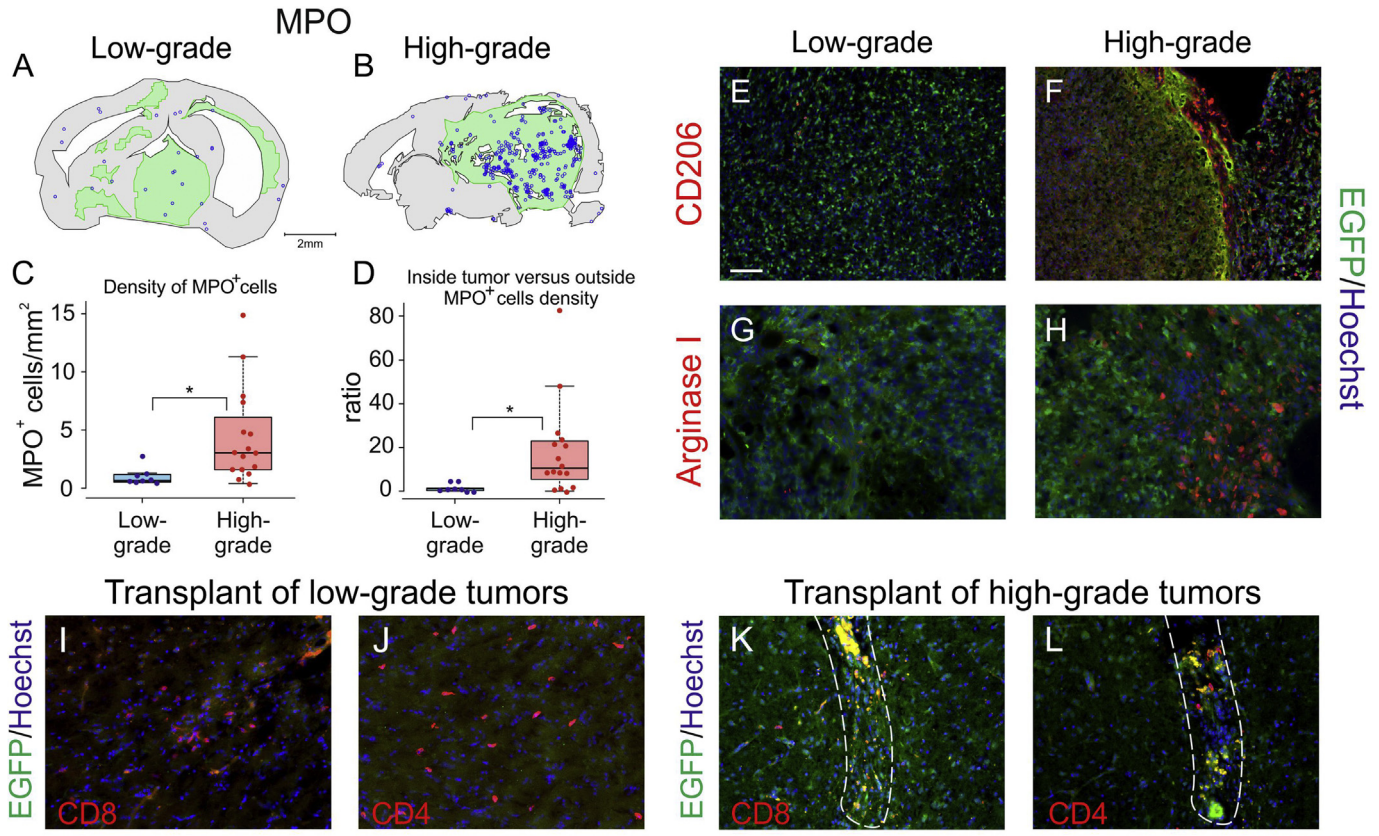

Fig. 4. Analysis of immune cells infiltration in glioma masses. A-B, Computer-assisted camera lucida drawing of brain sections stained with anti-GFP antibody to label tumor areas (green) and anti-MPO antibody labelling granulocytes (blue dots). Scale bar: 2 mm. C-D, Box plots show the density of MPO-positive cells in the brain sections (C) and the ratio between the density of MPO-positive cells inside the tumor versus that of the remaining healthy parenchyma (D). E-H, immunofluorescence stainings of low-grade (E,G) and high-grade (F,H) gliomas with anti-GFP antibody labelling tumor cells (in green), anti-CD206-or anti-Arginase-I antibody as indicated labelling immune-modulatory M2 cells (in red) that are enriched in high-grade gliomas. (I–L) Immunofluorescence stainings of sections of adult brains 14 days after the injection of low-grade (I–J) or high-grade (K–L) glioma cells using anti-GFP antibody labelling transplanted tumor cells (in green), anti-CD8 or anti-CD4 antibody as indicated (in red). While numerous lymphocytes infiltrate brains transplanted with low-grade glioma cells, very few lymphocytes are found in the areas surrounding the injection site (dashed lines in K,L) after high-grade glioma cells transplantation. The yellow signal is due to autofluorescence from necrotic cells inside the injection site. In all immunofluorescence micrographs nuclei were labelled with Hoechst 33342 (in blue). Scale bar: 100 μm (E–F), 50 μm (G–L). (For interpretation of the references to colour in this figure legend, the reader is referred to the Web version of this article.)

grown in NOD/SCID mice display levels more closely resembling those typical of high-grade fully progressed tumors arising in immunocompetent mice compared to the secondary tumors they originated from (Fig. 6A). Accordingly, the gene annotation enrichment analysis performed on all the differentially expressed genes in the comparison between secondary and tertiary tumors showed that, even in the progression occurring in NOD/SCID mice, the downregulated genes belonged to functional classes related to immune response and innate immunity activation (Fig. 6B).

To further substantiate the analysis, an unbiased expression profile comparison was performed between the four types of samples (low- and high-grade primary tumors, secondary and tertiary tumors induced by serial transplantation of low-grade tumors in NOD/SCID). In particular, we used PAM [33] to identify a group of genes whose expression enable the recognition of the four tumor types. A hierarchical clustering of such genes showed three main subgroups: one expressed at high level in all primary tumors, one expressed at high level in NOD/SCID transplants (both secondary and tertiary) and one highly expressed in low grade primary tumors and NOD/SCID secondary gliomas and poorly expressed in high grade primary tumors and tertiary gliomas. Gene ontology enrichment analysis showed that the first group do not display any coherent functional relationship; in the second group, the only significantly enriched GoTerm clusters are related to protein synthesis and oxidative phosphorylation, possibly indicating a more active metabolism. Strikingly, the third group was constituted by genes clearly sharing immunostimulatory features, confirming the results obtained from the previous analysis (Supplementary Fig. 5 and Supplementary Table 5).

4. Discussion

Somatic gene transfer of PDGF-B in neural progenitor cells represents a well-known model of glioma [34–36]. In our previous works, we showed that, although counter-intuitively, gliomas eliciting neurological symptoms at earlier time (i.e. from P30 to P60) appear to be less malignant than those that arise later. By analyzing at around P30 the brain of mice transduced at embryonic stages with PDGF-B, we demonstrated that all of them harbor multifocal gliomas. These gliomas, independently of having or not already caused neurological symptoms, are not able to propagate as tumors following transplantation in the brain of adult syngeneic mice, even when transplanted in a tenfold higher number compared to the saturating amount required for successful growth of high-grade tumor cells. This demonstrates that all gliomas, including those fated to emerge as high-grade grade tumors after longer latency, are initially characterized by lower malignancy and suggests that the early symptom onset of some tumors could be more related to the location of certain tumor foci rather than other intrinsic features. Supporting this view, is the observation that gliomas inducing symptoms at early stages are associated with hydrocephalus in about one third of the cases. The majority of the gliomas inducing

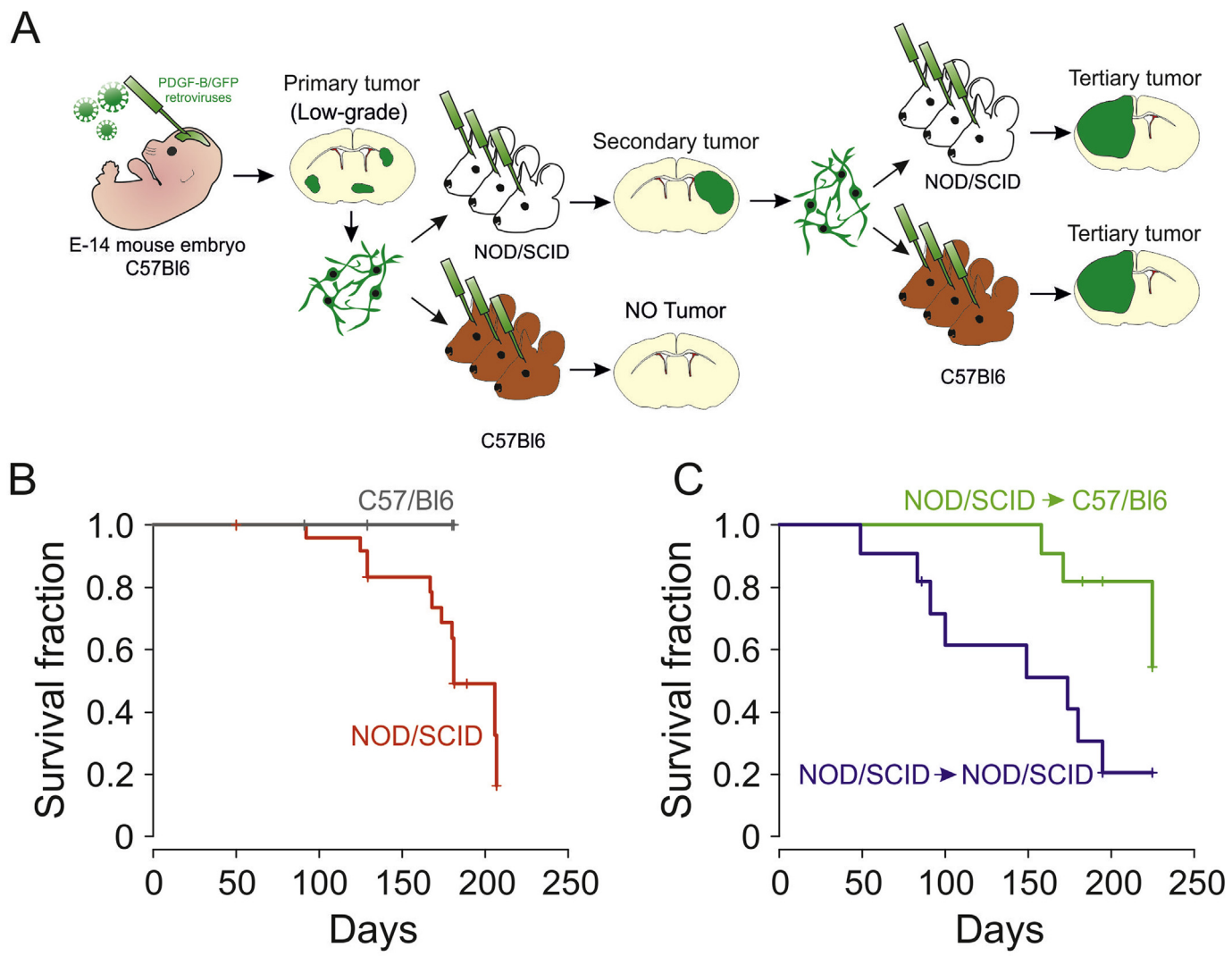

Fig. 5. Transplantation of low-grade glioma cells in adult mice. A, experimental design of serial transplantation of early onset/low-grade gliomas in NOD/SCID or C57BL/6 syngeneic mice to test the role of the immune system in counteracting glioma growth during the early step of gliomagenesis. B, Kaplan-Meier survival curves of C57BL/6 (gray line) or NOD/SCID (red line) mice transplanted with early onset/low-grade tumor cells show that low-grade gliomas are able to propagate in NOD/SCID mice. C, Kaplan-Meier survival curves of C57BL/6 (green line) or NOD/SCID (blue line) mice show that cells derived from secondary tumors that grew in NOD/SCID mice are able to propagate as tertiary tumors even in an immunocompetent mouse background. (For interpretation of the references to colour in this figure legend, the reader is referred to the Web version of this article.)

symptoms at a later time appears to have progressed towards a more malignant status, associated with the acquisition of tumor-propagating ability when transplanted. The analysis of the gene expression profiles of cells derived from low and high-grade gliomas highlights the prominent involvement of genes that play a role in the stimulation of immune system response, which are strongly downregulated in the high-grade ones. Considering that several glial components are known to establish a positive feedback loop when exposed to an inflammatory stimulus, thereby amplifying the immune system response [37–39], we can speculate that glioma progression may consist, at least in part, of the loss of this feedback mechanisms, thus acquiring immunoevasive abilities.

A clear difference between low- and high-grade gliomas is the composition of their immune infiltrate. We found that low-grade gliomas are extensively infiltrated by cytotoxic CD8 lymphocytes, which are instead rarely observed in high-grade gliomas. This observation gives a new contribution to the controversy about the significance of glioma-infiltrating CD8 lymphocytes: some authors reported that glioblastomas show higher CD8 infiltration than lower grade gliomas [40]. Other authors showed a negative correlation between CD8 infiltration and glioma grade [27]. It is worth to notice, however, that while the latter and our report examined the whole CD8 infiltrate, the former focused on perivascular CD8-positive lymphocytes which could be related to the stronger remodeling of blood vessel in glioblastoma. An additional change in the infiltrate composition occurring during the acquisition of tumor-propagating potential is the increase of granulocytes and macrophage/microglial cells expressing markers of immunomodulatory phenotypes. All these differences are not likely due to a difference in the maturity of the immune system of the tumor-bearing mice. No major differences in the maturation of the immune system of mice occurs between P30 and P180 [41]. A more likely interpretation is that at early stages gliomas possess immunogenic features that are gradually lost under the selective pressure of the immune system itself. Gliomas whose localization induces neurological symptoms at early stages likely still retain their immunostimulatory features and when transplanted in an immunocompetent adult mouse cause an immune response and fail to graft. On the contrary, transplantation in immunodeficient hosts does not result in rejection and secondary tumors eventually grow. The NOD/SCID immune environment likely does not exert the same

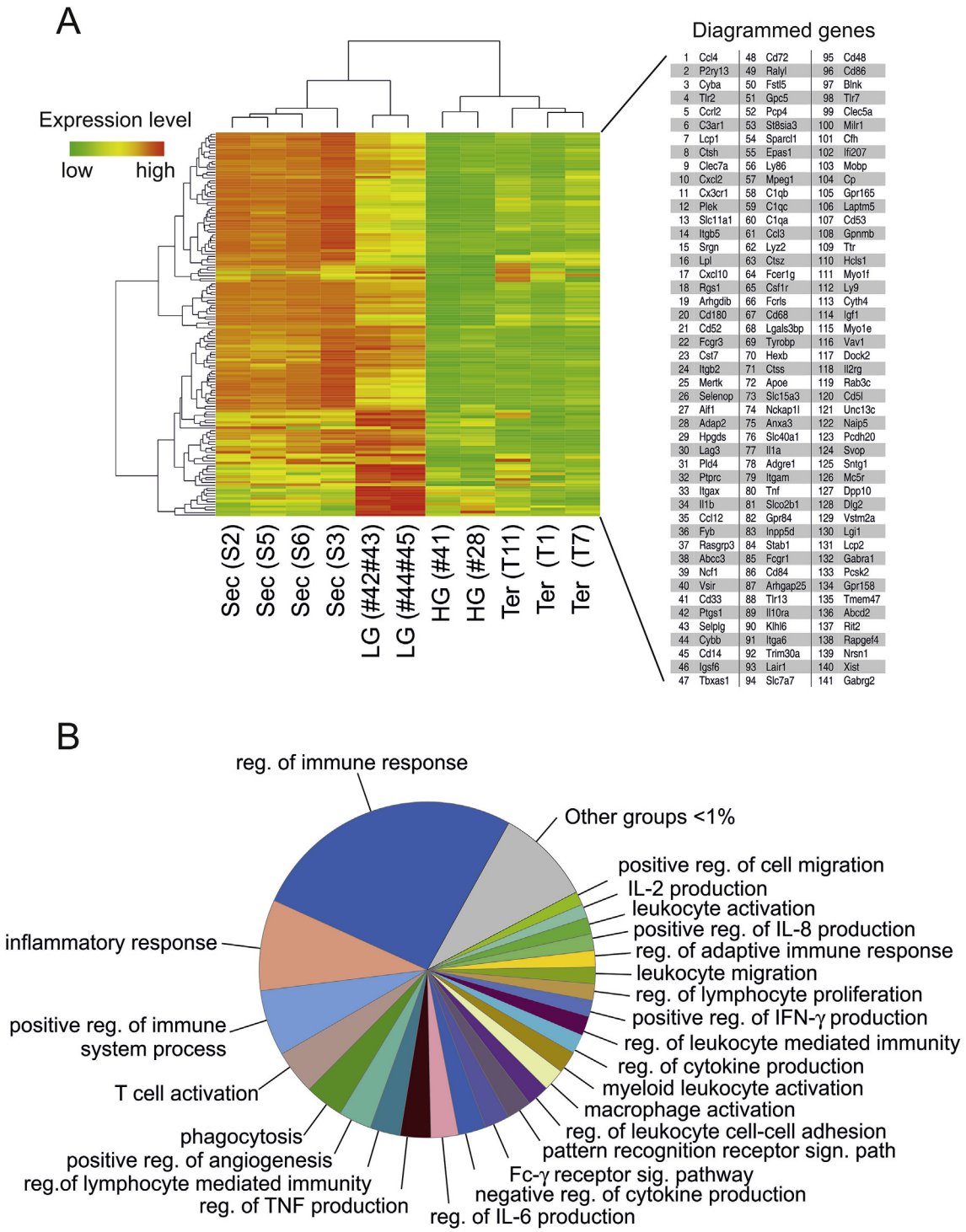

Fig. 6. Gene expression analysis of glioma cells. A, heatmap of the expression level of the immunostimulatory genes down-regulated during progression in the indicated samples. Primary (low-grade and high-grade) tumors derived from a C57Bl/6 background; Secondary and tertiary tumors were hosted in NOD/SCID background. B, Pie chart of GoTerm enrichment analysis of the genes down-regulated between secondary and tertiary tumors grown in NOD/SCID mice showing a strong enrichment in immune system related genes.

selective pressure on tumor cells allowing the retention of strongly immunostimulatory features as observed by their gene expression profile. To some extent, however, the residual immune system components found in NOD/SCID mice, mostly macrophages and granulocytes, is likely to eventually allow a progression towards higher grades of malignancy since these tumors became able to grow in immunocompetent adult mice. All in all, the data we present reveals the strong impact the immune system has on temporal patterns of progression to malignancy, pointing to roles for both main branches of the immune system.

Funding

This work was supported by Compagnia di San Paolo, Turin, Italy [grant number 2015.9834]; The European Research Counsil [ERC Grant number 340060]; The Italian Ministry of Health [grant number GR-

2011-02349694].

Conflicts of interest

The authors declare they have no conflicts of interest.

Acknowledgments

We thank Dr. Antonio Daga (Ospedale Policlinico San Martino – Genova, Italy) for helpful discussion on glioma progression. We are grateful to Dr. Filippo Calzolari (Johannes Gutenberg – Universität Mainz, Germany) for helpful comments on the manuscript. We would like to thank Dr. Michela Croce, Dr. Silvano Ferrini, Dr. Maria Pia Pistillo, Dr. Alessandro Poggi and Dr. Anna Rubartelli (Ospedale Policlinico San Martino – Genova, Italy) for invaluable suggestions on immunoediting mechanisms.

Appendix A. Supplementary data

Supplementary data to this article can be found online at https://doi.org/10.1016/j.canlet.2018.10.006.

References

[1] G.P. Dunn, A.T. Bruce, H. Ikeda, L.J. Old, R.D. Schreiber, Cancer immunoediting: from immunosurveillance to tumor escape, Nat. Immunol. 3 (2002) 991–998.
[2] G.P. Dunn, P.E. Fecci, W.T. Curry, Cancer immunoediting in malignant glioma, Neurosurgery 71 (2012) 201–222 discussion 222-203.
[3] R. Kim, M. Emi, K. Tanabe, Cancer immunoediting from immune surveillance to immune escape, Immunology 121 (2007) 1–14.
[4] J.B. Swann, M.J. Smyth, Immune surveillance of tumors, J. Clin. Invest. 117 (2007) 1137–1146.
[5] D. Mittal, M.M. Gubin, R.D. Schreiber, M.J. Smyth, New insights into cancer immunoediting and its three component phases–elimination, equilibrium and escape, Curr. Opin. Immunol. 27 (2014) 16–25.
[6] C.M. Koebel, W. Vermi, J.B. Swann, N. Zerafa, S.J. Rodig, L.J. Old, M.J. Smyth, R.D. Schreiber, Adaptive immunity maintains occult cancer in an equilibrium state, Nature 450 (2007) 903–907.
[7] K.K. Goswami, T. Ghosh, S. Ghosh, M. Sarkar, A. Bose, R. Baral, Tumor promoting role of anti-tumor macrophages in tumor microenvironment, Cell. Immunol. 316 (2017) 1–10.
[8] S. Pellegatta, L. Cuppini, G. Finocchiaro, Brain cancer immunoediting: novel examples provided by immunotherapy of malignant gliomas, Expet Rev. Anticancer Ther. 11 (2011) 1759–1774.
[9] I.M. Svane, A.M. Engel, M.B. Nielsen, H.G. Ljunggren, J. Rygaard, O. Werdelin, Chemically induced sarcomas from nude mice are more immunogenic than similar sarcomas from congenic normal mice, Eur. J. Immunol. 26 (1996) 1844–1850.
[10] A.M. Engel, I.M. Svane, J. Rygaard, O. Werdelin, MCA sarcomas induced in scid mice are more immunogenic than MCA sarcomas induced in congenic, immunocompetent mice, Scand. J. Immunol. 45 (1997) 463–470.
[11] V. Shankaran, H. Ikeda, A.T. Bruce, J.M. White, P.E. Swanson, L.J. Old, R.D. Schreiber, IFNgamma and lymphocytes prevent primary tumour development and shape tumour immunogenicity, Nature 410 (2001) 1107–1111.
[12] I. Benhar, A. London, M. Schwartz, The privileged immunity of immune privileged organs: the case of the eye, Front. Immunol. 3 (2012) 296.
[13] M.J. Carson, J.M. Doose, B. Melchior, C.D. Schmid, C.C. Ploix, CNS immune privilege: hiding in plain sight, Immunol. Rev. 213 (2006) 48–65.
[14] T. Oh, S. Fakurnejad, E.T. Sayegh, A.J. Clark, M.E. Ivan, M.Z. Sun, M. Safaee, O. Bloch, C.D. James, A.T. Parsa, Immunocompetent murine models for the study of glioblastoma immunotherapy, J. Transl. Med. 12 (2014) 107.
[15] I. Appolloni, F. Calzolari, E. Tutucci, S. Caviglia, M. Terrile, G. Corte, P. Malatesta, PDGF-B induces a homogeneous class of oligodendrogliomas from embryonic neural progenitors, Int. J. Canc. 124 (2009) 2251–2259.
[16] F. Calzolari, I. Appolloni, E. Tutucci, S. Caviglia, M. Terrile, G. Corte, P. Malatesta, Tumor progression and oncogene addiction in a PDGF-B-induced model of gliomagenesis, Neoplasia 10 (2008) 1373–1382 following 1382.
[17] M. Terrile, I. Appolloni, F. Calzolari, R. Perris, E. Tutucci, P. Malatesta, PDGF-B-driven gliomagenesis can occur in the absence of the proteoglycan NG2, BMC Canc. 10 (2010) 550.
[18] E. Gambini, E. Reisoli, I. Appolloni, V. Gatta, G. Campadelli-Fiume, L. Menotti, P. Malatesta, Replication-competent herpes simplex virus retargeted to HER2 as therapy for high-grade glioma, Mol. Ther.: J. Am. Soc. Gene Ther. 20 (2012) 994–1001.
[19] W. Huber, V.J. Carey, R. Gentleman, S. Anders, M. Carlson, B.S. Carvalho, H.C. Bravo, S. Davis, L. Gatto, T. Girke, R. Gottardo, F. Hahne, K.D. Hansen, R.A. Irizarry, M. Lawrence, M.I. Love, J. MacDonald, V. Obenchain, A.K. Oles, H. Pages, A. Reyes, P. Shannon, G.K. Smyth, D. Tenenbaum, L. Waldron, M. Morgan, Orchestrating high-throughput genomic analysis with Bioconductor, Nat. Methods 12 (2015) 115–121.
[20] B.M. Bolstad, R.A. Irizarry, M. Astrand, T.P. Speed, A comparison of normalization methods for high density oligonucleotide array data based on variance and bias, Bioinformatics 19 (2003) 185–193.
[21] G. Bindea, B. Mlecnik, H. Hackl, P. Charoentong, M. Tosolini, A. Kirilovsky, W.H. Fridman, F. Pages, Z. Trajanoski, J. Galon, ClueGO: a Cytoscape plug-in to decipher functionally grouped gene ontology and pathway annotation networks, Bioinformatics 25 (2009) 1091–1093.
[22] P. Shannon, A. Markiel, O. Ozier, N.S. Baliga, J.T. Wang, D. Ramage, N. Amin, B. Schwikowski, T. Ideker, Cytoscape: a software environment for integrated models of biomolecular interaction networks, Genome Res. 13 (2003) 2498–2504.
[23] R. Breitling, P. Armengaud, A. Amtmann, P. Herzyk, Rank products: a simple, yet powerful, new method to detect differentially regulated genes in replicated microarray experiments, FEBS Lett. 573 (2004) 83–92.
[24] W. Huang da, B.T. Sherman, R.A. Lempicki, Systematic and integrative analysis of large gene lists using DAVID bioinformatics resources, Nat. Protoc. 4 (2009) 44–57.
[25] W. Huang da, B.T. Sherman, R.A. Lempicki, Bioinformatics enrichment tools: paths toward the comprehensive functional analysis of large gene lists, Nucleic Acids Res. 37 (2009) 1–13.
[26] S. Hadrup, M. Donia, P. Thor Straten, Effector CD4 and CD8 T cells and their role in the tumor microenvironment, Cancer Microenviron 6 (2013) 123–133.
[27] S. Han, C. Zhang, Q. Li, J. Dong, Y. Liu, Y. Huang, T. Jiang, A. Wu, Tumour-infiltrating CD4(+) and CD8(+) lymphocytes as predictors of clinical outcome in glioma, Br. J. Canc. 110 (2014) 2560–2568.
[28] P. Gravelle, C. Do, C. Franchet, S. Mueller, L. Oberic, L. Ysebaert, L.M. Larocca, S. Hohaus, M.N. Calmels, F.X. Frenois, R. Kridel, R.D. Gascoyne, G. Laurent, P. Brousset, S. Valitutti, C. Laurent, Impaired functional responses in follicular lymphoma CD8(+)TIM-3(+) T lymphocytes following TCR engagement, OncoImmunology 5 (2016) e1224044.
[29] R.A. Jonas, T.F. Yuan, Y.X. Liang, J.B. Jonas, D.K. Tay, R.G. Ellis-Behnke, The spider effect: morphological and orienting classification of microglia in response to stimuli in vivo, PloS One 7 (2012) e30763.
[30] A. Sierra, F. de Castro, J. Del Rio-Hortega, J. Rafael Iglesias-Rozas, M. Garrosa, H. Kettenmann, The "Big-Bang" for modern glial biology: translation and comments on Pio del Rio-Hortega 1919 series of papers on microglia, Glia 64 (2016) 1801–1840.
[31] I. Mishalian, R. Bayuh, L. Levy, L. Zolotarov, J. Michaeli, Z.G. Fridlender, Tumor-associated neutrophils (TAN) develop pro-tumorigenic properties during tumor progression, Cancer Immunol. Immunother.: CII 62 (2013) 1745–1756.
[32] K.S. Siveen, G. Kuttan, Role of macrophages in tumour progression, Immunol. Lett. 123 (2009) 97–102.
[33] R. Tibshirani, T. Hastie, B. Narasimhan, G. Chu, Diagnosis of multiple cancer types by shrunken centroids of gene expression, Proc. Natl. Acad. Sci. U. S. A. 99 (2002) 6567–6572.
[34] F. Calzolari, P. Malatesta, Recent insights into PDGF-induced gliomagenesis, Brain Pathol. 20 (2010) 527–538.
[35] E.I. Fomchenko, E.C. Holland, Mouse models of brain tumors and their applications in preclinical trials, Clin. Canc. Res.: Off. J. Am. Assoc. Canc. Res. 12 (2006) 5288–5297.
[36] A.H. Shih, E.C. Holland, Platelet-derived growth factor (PDGF) and glial tumorigenesis, Cancer Lett. 232 (2006) 139–147.
[37] C. Farina, F. Aloisi, E. Meinl, Astrocytes are active players in cerebral innate immunity, Trends Immunol. 28 (2007) 138–145.
[38] S. van Neerven, A. Nemes, P. Imholz, T. Regen, B. Denecke, S. Johann, C. Beyer, U.K. Hanisch, J. Mey, Inflammatory cytokine release of astrocytes in vitro is reduced by all-trans retinoic acid, J. Neuroimmunol. 229 (2010) 169–179.
[39] C. Rosenbaum, M.A. Schick, J. Wollborn, A. Heider, C.J. Scholz, A. Cecil, B. Niesler, J. Hirrlinger, H. Walles, M. Metzger, Activation of myenteric glia during acute inflammation in vitro and in vivo, PloS One 11 (2016) e0151335.
[40] I. Yang, S.J. Han, M.E. Sughrue, T. Tihan, A.T. Parsa, Immune cell infiltrate differences in pilocytic astrocytoma and glioblastoma: evidence of distinct immunological microenvironments that reflect tumor biology, J. Neurosurg. 115 (2011) 505–511.
[41] K.S. Landreth, Critical windows in development of the rodent immune system, Hum. Exp. Toxicol. 21 (2002) 493–498.